ENVIRONMENTAL RESEARCH
LETTERS

PURPOSE-LED PUBLISHING™

Part of the
ENVIRONMENTAL RESEARCH
SERIES

LETTER • **OPEN ACCESS**

Unraveling the response of the apparent temperature sensitivity of ecosystem respiration to rising temperature

To cite this article: Zhentao Liu *et al* 2025 *Environ. Res. Lett.* **20** 034008

IOP Publishing Environ. Res. Lett. 20 (2025) 034008 https://doi.org/10.1088/1748-9326/adad00

ENVIRONMENTAL RESEARCH
LETTERS

OPEN ACCESS

RECEIVED
29 August 2024

REVISED
31 December 2024

ACCEPTED FOR PUBLICATION
22 January 2025

PUBLISHED
11 February 2025

LETTER

Unraveling the response of the apparent temperature sensitivity of ecosystem respiration to rising temperature

Zhentao Liu[1], **Junguo Liu**[1,2,3,*] **and Deliang Chen**[4,5]

[1] School of Environmental Science and Engineering, Southern University of Science and Technology, Shenzhen 518055, People's Republic of China
[2] Yellow River Research Institute, North China University of Water Resource and Electric Power, Zhengzhou 450046, People's Republic of China
[3] Henan Provincial Key Laboratory of Hydrosphere and Watershed Water Security, North China University of Water Resource and Electric Power, Zhengzhou 450046, People's Republic of China
[4] Department of Earth System Sciences, Tsinghua University, Beijing 100084, People's Republic of China
[5] Department of Earth Sciences, University of Gothenburg, S-40530 Gothenburg, Sweden
[*] Author to whom any correspondence should be addressed.

E-mail: junguo.liu@gmail.com

Keywords: ecosystem respiration, rising temperature, short-term warming, non-temperature factors, seasonality

Supplementary material for this article is available online

Abstract

Global warming is expected to intensify carbon loss, as ecosystem respiration (RECO) rates increase exponentially with rising temperatures. However, a comprehensive analysis of the response of the apparent temperature sensitivity of RECO (Q_{10}) to rising temperature is lacking. This study leverages observational data from 254 sites from the FLUXNET2015 and AmeriFlux datasets to address this knowledge gap. We found a strong influence of non-temperature factors on the seasonality of RECO. The similar seasonality of this effect and temperature can lead to underestimating or overestimating Q_{10}. In this study, Q_{10} was quantified using a temporal moving window and a linear-mixed effect model to account for the effects of non-temperature factors on RECO. Our results show that Q_{10} decreases from 1.55 ± 0.24 (mean ± one standard error) at 5 °C to 1.35 ± 0.18 at 25 °C over all sites. The mean slope of Q_{10} to temperature across all sites is about $-0.02\ ^{\circ}\mathrm{C}^{-1}$. In this study, we found lower values of Q_{10} and a lower decreasing rate of Q_{10} with rising temperature compared to previous studies. Our study suggests that Q_{10} might be systematically overestimated due to the confounding effect of non-temperature factors, potentially leading to overestimated simulation of RECO rate. Our study also emphasizes the necessity of developing a process-based model, rather than simply incorporating the influences of non-temperature factors into Q_{10}.

1. Introduction

The response of the biosphere to global warming has garnered significant attention due to the crucial role terrestrial ecosystems play in regulating the global carbon cycle and atmospheric carbon dioxide (CO_2) concentration (Dow *et al* 2022, Tang *et al* 2022, Zhang *et al* 2023). Ecosystem respiration (RECO), as the primary source of CO_2 emissions from terrestrial ecosystems, determines the carbon balance of ecosystems in conjunction with gross primary production (Yu *et al* 2022). Increasing temperature is expected to accelerate the RECO rate, stimulating additional CO_2 emissions (Chen *et al* 2021). Intrinsic temperature sensitivity describes the response of inherent kinetic properties to ambient temperature (Davidson and Janssens 2006). The apparent temperature sensitivity of RECO (Q_{10}), which represents the proportional increase in RECO rate per 10 °C rise in temperature under environmental constraints (Davidson and Janssens 2006, Niu *et al* 2021, Sun *et al* 2023), is an important parameter commonly used in modeling the RECO rate. Knowing how Q_{10} evolves with global warming is critical for understanding the direction and magnitude of carbon-climate feedback (Chen *et al* 2021, Johnston *et al* 2021).

A recent study based on this method found a homogenization in Q_{10} in a warming world (Niu *et al* 2021). However, this global analysis is still incomplete since the influence of non-temperature factors on RECO is not accounted for. Seasonal variation in RECO can be influenced by temperature, as well as biomass, ecosystem structure, and substrate availability, all of which also exhibit seasonal fluctuations (Brown *et al* 2004, Jia *et al* 2014). For instance, about 50% of total plant respiration comes from leaves (Slot and Kitajima 2015), and the seasonal variation in RECO rate can be partially attributed to leaf phenology. This oversight could misattribute seasonal fluctuations in RECO rates entirely to temperature changes, potentially leading to an underestimation or overestimation of Q_{10}. This issue might also clarify the high variability in Q_{10} values observed across different ecosystems and seasons, ranging from as low as 1.0 to as large as 9.0 (Demyan *et al* 2016, Mu *et al* 2017, Yang *et al* 2022, Zhang *et al* 2024).

Moreover, global warming has led to irreversible transformations within ecosystems worldwide, substantially impacting RECO. Vegetation greening, growing season prolongation, and exacerbated atmospheric water vapor pressure deficit can affect above-ground RECO by altering ecosystem structure, biomass, and carbohydrate supply (McDowell and Allen 2015, Yuan *et al* 2019, Grossiord *et al* 2020, Liu *et al* 2020, Yan *et al* 2024). Permafrost melting, soil texture change, and phosphorus and nitrogen content variation can affect below-ground RECO (Pries *et al* 2015, Bond-Lamberty *et al* 2024, Chen *et al* 2024). Therefore, previous quantification of Q_{10} without excluding the influence of non-temperature factors might lead to large uncertainty in predicting RECO in a warming world.

Previous studies commonly overlook the role of non-temperature factors when calculating Q_{10} values. Therefore, we first investigated the effect of non-temperature factors on RECO and its disturbance on calculated Q_{10}. Our objective is to quantify Q_{10} while excluding the confounding effect of non-temperature factors and to evaluate the impact of rising temperature on Q_{10}. A temporal moving window and linear-mixed effect model were used to exclude the non-temperature effects on RECO while calculating Q_{10}. In this context, the term 'rising temperature' merely refers to short-term warming, specifically within a period of less than 15 d, as determined by the size of our temporal moving window. Due to the limited duration of observations, the effects of long-term warming are beyond the scope of this study. The availability of continuous hourly or half-hourly eddy covariance observations from flux towers, along with a wide range of temperatures, allows us to investigate the warming effect on Q_{10} based on site-level data.

2. Materials and methods

2.1. Eddy covariance data

We used hourly or half-hourly RECO rate and air temperature data from the AmeriFlux and FLUXNET2015 datasets (Chu *et al* 2023, Pastorello *et al* 2020). In case of overlap between different databases, the one with longer observation was chosen. We analyzed only those sites that provided at least 1 year of complete RECO rate and meteorological data (gaps $< 5\%$), 254 sites covered a wide range of temperatures and ecosystem types were preserved (figures 1(a) and (b)). Both AmeriFlux dataset and FLUXNET2015 dataset have undergone a standardized set of quality control and gap-filling. Only measured air temperature data and gap-filled air temperature data with good quality ($QC = 0$ or $QC = 1$) and nighttime net ecosystem exchange (NEE) data (incoming shortwave radiation potential is equal to 0) were used in this study to ensure the reliability of our results. To ensure enough sampled data, measured NEE data and gap-filled NEE data with good and medium quality were used in this study.

2.2. Calculation of Q_{10}

The Van't Hoff function (Mahecha *et al* 2010) for RECO rate is given as,

$$R = R_{\mathrm{ref}} Q_{10}^{\frac{T - T_{\mathrm{ref}}}{10}}, \tag{1}$$

where R is the RECO rate, R_{ref} is the reference RECO rate at T_{ref}, and T_{ref} is the reference temperature, in this study, 10 °C is chosen as T_{ref}; Q_{10} is the RECO temperature sensitivity.

The air temperature and RECO rate data used for calculating Q_{10} were sampled in the following steps. First, data sampling was conducted in a 15 d moving window to minimize the effect of non-temperature factors on the seasonal variation in RECO rate. Then, a 10 °C window with a 2 °C step size was used to capture the effect of air T on; the Q_{10} calculated in a given window was considered to be the Q_{10} at the median T of the temperature window. Temperature data with a difference of <6 °C between the 90th and 10th percentiles were excluded. Note that this sampling procedure was conducted for each site.

We calculated the apparent temperature sensitivity of RECO using a linear transformation of the Van't Hoff function with a linear mixed-effect model (Li *et al* 2023) each site and each temperature window,

$$\begin{aligned} \ln R_{i,j} = {} & \left(\overline{\ln Q_{10,i,j}} + \ln \varepsilon^{k}_{Q_{10,i,j}}\right)\left(\frac{T - T_{\mathrm{ref}}}{10}\right) \\ & + \overline{\ln R_{\mathrm{ref},i,j}} + \ln \varepsilon^{k}_{R_{\mathrm{ref},i,j}}, \end{aligned} \tag{2}$$

where, $R_{i,j}$ is the RECO rate in temperature window j (I_j) at site i (S_i), $R_{\mathrm{ref},i,j}$ is the reference RECO rate at reference temperature $\mathrm{T}_{\mathrm{ref}}$ in I_j at S_i, and $\overline{Q_{10,i,j}}$ is the

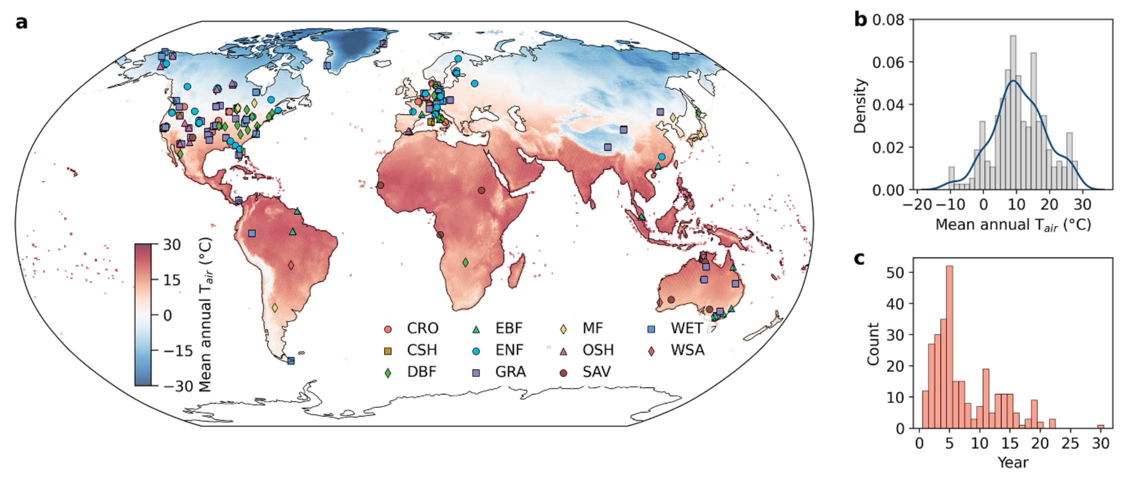

Figure 1. Studied sites cover a wide range of temperature and ecosystem types. (a) The spatial distribution of studied sites, the base map is the mean annual air temperature derived from the CRU monthly mean temperature dataset from 1971 to 2022. The colored points represent ecosystem types. (b) The density distribution of the mean annual air temperature of all flux stations that were used in this study. (c) Temporal distribution of observation years across all sites. See the full name of the ecosystem type in table S1.

mean temperature sensitivity across all temporal windows numbered by k in I_j at S_i. R_{ref} is the RECO rate at a constant temperature, thus, the change in R_{ref} is caused by non-temperature factors. In equation (2), the non-temperature effects were excluded in the linear mixed-effects model by treating the intercept as a random variable with averages of $\overline{\ln R_{\text{ref}}}$ and defining $\varepsilon^k_{R_{\text{ref},i,j}}$ in I_j at S_i as temporal window-specific deviation from these averages, while $\varepsilon^k_{Q_{10,i,j}}$ is the $Q_{10,i,j}$ deviation. Linear mixed-effects modeling was conducted using the R package 'lmer' (Bates *et al* 2015).

2.3. Quantification of the effect of non-temperature factors on the seasonality of RECO

RECO rate at a constant temperature (T_{c}), can be used as an indicator for detecting non-temperature effects. The choice of T_{c} was based on the climate conditions of specific sites to capture the seasonal change in R_{Tc}. T_{c} is 10 °C for sites with mean annual air temperature ($T_{\text{site},m}$) lower than 10 °C, and it is 15 °C for sites with $T_{\text{site},m}$ greater than 10 °C but below 15 °C, while it is 20 °C for other sites. The ratio between the amplitude of seasonal variation in monthly mean R_{Tc} ($R_{\text{Tc,mon}}$) and the amplitude of seasonal variation in monthly mean RECO rate (R_{mon}) was calculated for each site and each year. The difference between maximum and minimum $R_{\text{Tc,mon}}$ (R_{mon}) within a year is the amplitude of the seasonal variation in $R_{\text{Tc,mon}}$ (R_{mon}), i.e $\Delta R_{\text{Tc,mon}}$ (ΔR_{mon}). There are some missing values for $R_{\text{Tc,mon}}$ because of high seasonal change in air temperature, only temporally overlapped values were reserved.

2.4. Quantification of the coupling between R_{Tc} and temperature

The coupling between R_{Tc} and temperature was detected at each site and each year. First, the median of all temperature data for a site was chosen as the constant temperature. Then, the mean of temperatures in a 15 d moving window and the mean RECO rate at a constant temperature (T_{c}, with a variation of ±0.5 °C to ensure sufficient data sampling) in a 15 d moving window were calculated. At last, Spearman's correlation was calculated to quantify the coupling between R_{Tc} and temperature.

Spearman's rank correlation was used to examine the coupling between R_{Tc} and temperature. The t-test was used to test the significance of each correlation coefficient. The optimal index fitting and simple linear regression between site mean annual temperature and Q_{10} is conducted in Python using the Scipy library (Virtanen *et al* 2020).

3. Results

3.1. The role of non-temperature factors in seasonality of RECO

The seasonal variation of RECO rate can be affected by non-temperature factors. In figure 2(a), points 'a', 'b', and 'c' represent three distinct time points. Point 'a' corresponds to the earliest date, point 'c' to the latest date, and point 'b' is positioned at the same date as point 'c'. The temperatures at time points 'a' and 'b' are the same; therefore, the difference in the RECO rate between 'a' and 'c' can be attributed to two parts, temperature and no-temperature effects. The RECO rate at a constant temperature (R_{Tc}),

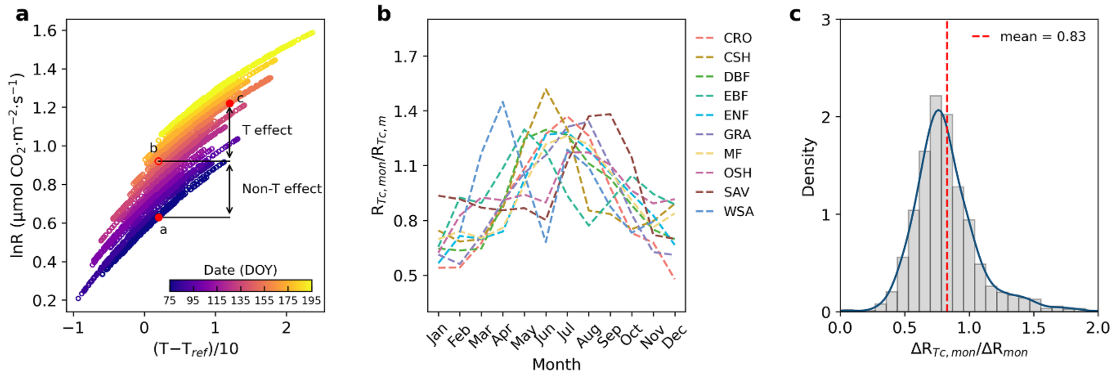

Figure 2. The seasonal variation of ecosystem respiration caused by non-temperature factors. (a) The schematic diagram shows the temperature effect and non-temperature effect on seasonal variation in RECO rate. The data is derived from site FR-Fon and its ecosystem type is deciduous broadleaf forest. (b) Seasonal change of $R_{\mathrm{Tc,mon}}/R_{\mathrm{Tc},m}$ across different ecosystem types in the northern hemisphere. The colors of the dashed lines represent ecosystem types. (c) The density distribution of the ratio between seasonal variation amplitude of $R_{\mathrm{Tc,mon}}$ ($\Delta R_{\mathrm{Tc,mon}}$) and seasonal variation amplitude of R_{mon} (ΔR_{mon}), the total number of site-year is 1647. The vertical red dashed line represents the mean ratio value.

was chosen to detect the effects of non-temperature factors on the seasonality of RECO rate. All ecosystem types in the Northern Hemisphere show a clear seasonal variation in $R_{\mathrm{Tc,mon}}$ (the mean value of R_{Tc} for a month), with the occurrence of peak and minimum values differing among ecosystem types (figure 2(b)). The normalized $R_{\mathrm{Tc,mon}}$ ($R_{\mathrm{Tc,mon}}/R_{\mathrm{Tc,m}}$, $R_{\mathrm{Tc,m}}$ is the mean of $R_{\mathrm{Tc,mon}}$ values within a year) ranges from 0.5 to 1.5. The peak value occurs commonly in summer (June to August), while the minimum typically occurs in winter, except in savannas. Notably, there are two peak values for woody savannas and evergreen broad-leaf forests. Similar seasonal variations in $R_{\mathrm{Tc,mon}}$ are also observed at sites in the Southern Hemisphere (figure S1), with differences in timing due to the reversed seasons compared to the Northern Hemisphere. Our results suggest that the seasonal pattern of $R_{\mathrm{Tc,mon}}$ closely mirrors that of temperature.

The seasonal variation in $R_{\mathrm{Tc,mon}}$ was compared with the seasonal variation in the monthly mean RECO rate (R_{mon}) by calculating the ratio between the amplitude of seasonal variation in $R_{\mathrm{Tc,mon}}$ ($\Delta R_{\mathrm{Tc,mon}}$) and the amplitude of seasonal variation in R_{mon} (ΔR_{mon}, see details in the method section). Our results show that the seasonal variation in R_{mon} is primarily governed by $R_{\mathrm{Tc,mon}}$, with a mean ratio of about 0.83 (figure 2(c)). It is important to note that this ratio might exceed 1.0 under specific conditions. This occur when the promoting effect of non-temperature factors, such as biomass and soil moisture, on RECO is low at high temperatures and reversed at low temperatures. For example, the negative correlation between temperature and precipitation can lead this ratio to exceed 1.0 in EBF (figure S2), as water availability plays a dominant role in RECO variation. Further analysis indicates that the dominant role of $R_{\mathrm{Tc,mon}}$ is more significant in arid regions than in other regions, with the exception of tropical regions (figure S2). Our results confirm the dominant role of $R_{\mathrm{Tc,mon}}$ in the seasonal variation of R_{mon}, implying that the methods for calculating Q_{10} in most previous studies (Tjoelker *et al* 2001, Fouché *et al* 2014, Johnston *et al* 2021, Niu *et al* 2021) might overestimate or underestimate Q_{10} values since they did not consider the impact of non-temperature factors, such as seasonal variation in substrates.

3.2. Impact of non-temperature factors on site-year Q_{10}

We then investigated the effect of the coupling between R_{Tc} and temperature on site-year Q_{10}, which is the Q_{10} calculated using full-year hourly or half-hourly air temperature and RECO rate data. The coupling between R_{Tc} and temperature was quantified based on Spearman's correlation coefficient. Results show that there is a strong positive coupling between temperature and R_{Tc} (figure 3(a)), Specifically, 57.9% of all site years demonstrated Spearman's correlation coefficients greater than 0.5 (out of a total of 1505 site-years). This effect was particularly pronounced in deciduous broad-leaf forests, evergreen needle-leaf forests, and mixed forests, where more than 60% of the correlation coefficients exceeded 0.5. Additionally, more than 50% of Spearman's correlation coefficients for cropland, closed shrubland, grassland, savanna, and wetland were also greater than 0.5. Conversely, woody savanna exhibited the highest negative coupling, with 32.4% of Spearman's correlation coefficients falling below −0.5.

The positive coupling was especially strong for temperate and continental sites (figure S3), likely because of the similar seasonal variation between temperature and R_{Tc} in these regions. This similar seasonal variation in temperature and R_{Tc} is due to the tight correlation between temperature and

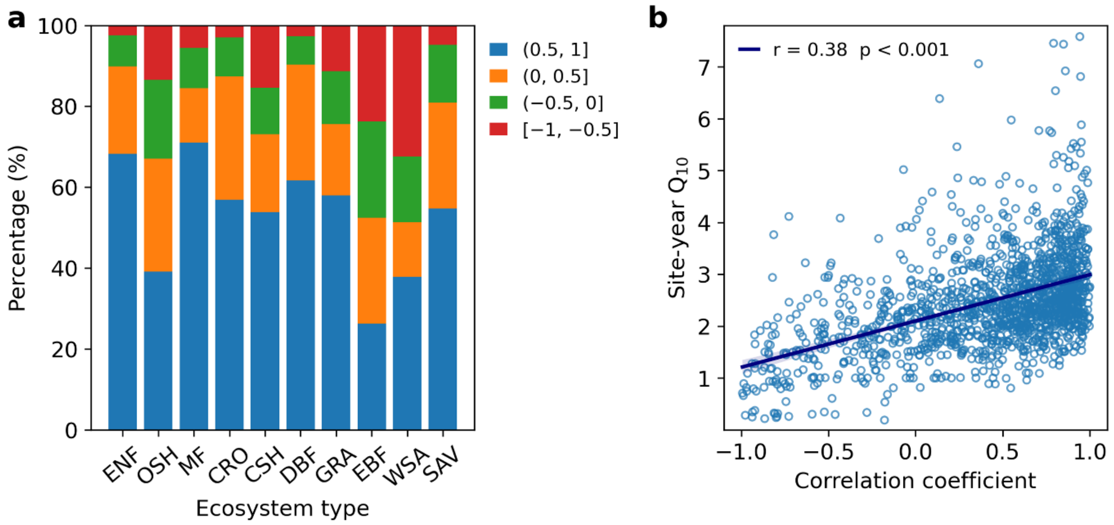

Figure 3. The relationship between site-year Q_{10} and the coupling between R_{Tc} and temperature. (a) The distribution of correlation coefficients between R_{Tc} and temperature for different ecosystem types, all correlation coefficient values are contained even without passing the significance test. The different colors represent different ranges of correlation coefficient values. Blue, orange, green, and red correspond to the intervals (0.5, 1], (0, 0.5], (−0.5, 0], and [−1, −0.5], respectively. (b) The relationship between site-year apparent temperature sensitivity and Spearman's correlation coefficient between R_{Tc} and temperature (see methods for details).

precipitation (figure S4), as both temperature and precipitation play a significant role in controlling plant phenology (Moles *et al* 2014), additionally, water availability can impact RECO substantially (Liu *et al* 2018, Zhang *et al* 2018). For example, positive correlations between precipitation and temperature were found in most CRO, CSH, ENF, GRA, MF, and SAV sites (figure S4), where positive coupling between R_{Tc} and temperature was also found. The negative coupling between R_{Tc} and temperature was found in sites that have negative correlations between temperature and precipitation, such as EBF and WSA. Further, we found a significant positive correlation between Q_{10} and the coupling between temperature and R_{Tc} ($r = 0.38$, $p < 0.001$) was found (figure 3(b)). As the correlation coefficient increased, Q_{10} rose from 0.89 ± 0.45 (mean ± one standard error) when $r < -0.9$, to 3.00 ± 0.98 when $r > 0.9$. These results suggest that the coupling between temperature and R_{Tc} within a year complicates the estimation of Q_{10}, highlighting the need to exclude the effect of seasonal change of R_{Tc}.

3.3. The response of Q_{10} to rising temperature

We quantified Q_{10} while minimizing the confounding influence of non-temperature effects by employing a temporal moving window and applying a linear mixed-effect model for each site and temperature window. Figure 2(a) shows that the effect of non-temperature factors on seasonality is obvious at the seasonal scale, with the time scale decreasing, the effect of non-temperature factors on change in RECO rate is negligible compared to temperature. Therefore, a 15 d moving window was used for data sampling to minimize the non-temperature effect on calculated Q_{10} (see details in the method section). Our results are consistent with previous studies (Tjoelker *et al* 2001, Johnston *et al* 2021), showing a decline in Q_{10} with short-term warming (figure 4(a), merely Q_{10} values with p-values less than 0.05 were considered). The mean value of Q_{10} decreases from 1.55 at 6 °C to 1.36 at 26 °C, with a decreasing rate of 0.01 per degree. However, our results show that the decreasing rate of Q_{10} with rising temperature is much slower than a previous study (Niu *et al* 2021), which found Q_{10} decreases from 2.4 at 9 °C to 1.8 at 17 °C. We further calculated the slope of Q_{10} to temperature for each site and categorized the slope values according to different ecosystem types (figure 4(b)). The results show that all ecosystem types except wetlands and mixed forests show relatively higher decreasing rates. Additionally, the slope values also show high variability with the same ecosystem type, such as evergreen needle forests and grassland. This high variability might be due to the difference in hydrothermal conditions across sites.

4. Discussion and conclusion

In this study, we found that non-temperature factors dominate the seasonality of the monthly mean of RECO rate and a strong coupling between R_{Tc} and temperature in a large number of the sites. This indicates that the effect of non-temperature factors will be attributed to the change in temperature if the effect of non-temperature factors on the RECO rate is not eliminated, leading to underestimations or overestimations of site-year Q_{10}. Therefore, we calculated after minimizing the confounding effect

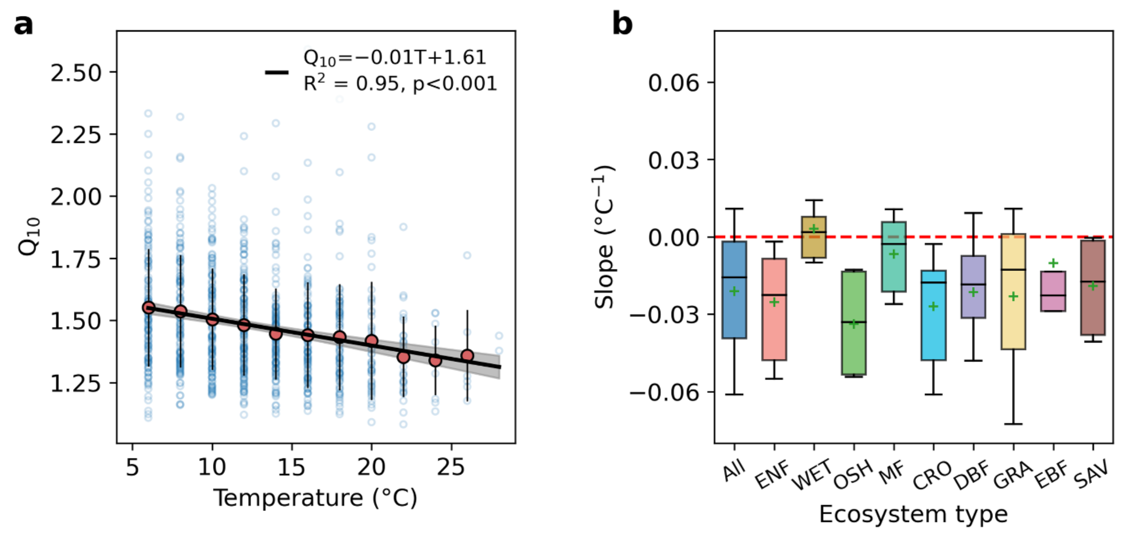

Figure 4. The response of Q_{10} to rising temperature. (a) The relationship between Q_{10} and T; the solid line is the linear regression line based on mean Q_{10} values, and the gray shaded area represents a 99% confidence interval. The red points represent mean values and the error bars correspond to one standard error. (b) The slope of Q_{10} to temperature for each site across different ecosystem types and the ecosystem type is sorted by temperature, with higher mean annual temperature on the right. The median slope value is represented by the black line in each box, while the mean value is represented by the green plus sign. The lower and upper whiskers correspond to the 10th and 90th percentiles, respectively.

of non-temperature factors on RECO rate, the Q_{10} values we calculated are smaller than those in previous studies (Demyan *et al* 2016, Mu *et al* 2017, Yang *et al* 2022, Zhang *et al* 2024). Consistent with previous studies, we found that Q_{10} decreases with rising temperature (Tjoelker *et al* 2001, Johnston *et al* 2021, Bruhn *et al* 2022). However, we found that the rate at which Q_{10} decreases with temperature is significantly slower than in a previous study (Niu *et al* 2021), which may be due to their overestimation of Q_{10} caused by not removing the effect of non-temperature factors. Several mechanisms have been proposed to explain the decline in Q_{10} with rising temperature, including biochemical changes, structural changes, and limitations on substrate availability (Atkin and Tjoelker 2003, Bradford *et al* 2008, Niu *et al* 2012).

A 15 d moving window was used for sampling data to minimize the confounding effect of non-temperature factors on Q_{10} in this research. Variations in non-temperature factors, including soil moisture (Brocca *et al* 2010), leaf area index, and biomass (Liu *et al* 2023), are considerably less pronounced at the sub-monthly scale than at seasonal or annual scales. This indicates that the impact of non-temperature factors on the RECO rate is minimal compared to that of temperature, effectively decoupling the influence of temperature from the influences of non-temperature factors on the RECO rate at the sub-monthly scale. A previous study investigated the impact of moving window size on Q_{10}, showing that Q_{10} calculated in a 15 d window is equivalent to that in a 7 d window (Reichstein *et al* 2005). This further suggests that the confounding effect of non-temperature factors on calculated Q_{10} is negligible within 15 d. Therefore, a 15 d moving window is capable of excluding the effect of non-temperature factors on Q_{10}. Evidence suggests that RECO responds differently to rising temperatures under different conditions (Li *et al* 2020), and thus Q_{10} may vary across different temporal windows. In this research, it should be noted that our calculated Q_{10} represents the mean Q_{10} under different conditions because a linear mixed effect model was used to calculate Q_{10} values.

In conclusion, this study provides significant insights into the impact of rising temperature on Q_{10}. Notably, we highlight the role of non-temperature factors in the seasonality of RECO and the importance of excluding their confounding effect when calculating Q_{10}. This underscores the necessity to explore the direct relationship between non-temperature factors—such as ecosystem biomass, substrate availability, and ecosystem structure—and RECO, rather than simply incorporating their effects into Q_{10}, in other words, their impacts on how RECO responds to rising temperatures. Our research reveals relatively lower Q_{10} values and a weaker negative effect of rising temperature on Q_{10} compared to previous studies (Demyan *et al* 2016, Mu *et al* 2017, Niu *et al* 2021, Yang *et al* 2022, Zhang *et al* 2024), suggesting that the increasing rate of RECO with rising temperature might have been overestimated in the past. Furthermore, the possibility of warming-carbon positive feedback in a warming world still involves large uncertainties, as global warming is altering water availability, ecosystem structure, and phenology (McDowell and Allen 2015, Yuan *et al* 2019, Grossiord *et al* 2020, Liu *et al* 2020, Yan *et al* 2024), which should also be considered in the warming-carbon feedback analysis. Moreover, it is necessary to investigate the impact of long-term warming on

Q_{10} for better understanding of the carbon-climate feedback as the global warming has been projected to continue in the coming decades (IPCC 2022).

Data availability statement

Python codes used to produce the results in this paper can be accessed at https://zenodo.org/records/14305789. CRU TS 4.07 data is obtained from https://crudata.uea.ac.uk/cru/data/hrg/.

The data that support the findings of this study are openly available at the following URL/DOI: https://fluxnet.org/; https://ameriflux.lbl.gov/.

Acknowledgment

This study has been supported by the National Natural Science Foundation of China (Grant No. 42361144001), the 111 Project (Grant No. D25014), the National Foreign Experts Program (Category S) (Grant No. S20240116), Henan Provincial Key Laboratory of Hydrosphere and Watershed Water Security, and the Henan Province Foreign Scientist Studio for Synergistic Management of Water, Food, Energy, and Carbon (Grant No. GZS2024013). This work was performed as part of the IAHS HELPING Working Group on *Stepwise Ecological Restoration of Watersheds* and on *Acceptance of Nature-based Solutions & Their Implementation in Guidelines*. DC was supported by the Swedish National Strategic programs BECC and MERGE.

ORCID iDs

Zhentao Liu https://orcid.org/0009-0008-2339-765X
Deliang Chen https://orcid.org/0000-0003-0288-5618

References

Atkin O K and Tjoelker M G 2003 Thermal acclimation and the dynamic response of plant respiration to temperature *Trends Plant Sci.* **8** 343–51

Bates D *et al* 2015 Package 'lme4' *Convergence* p 12 (available at: https://cran.r-project.org/web/packages/lme4/lme4.pdf)

Bond-Lamberty B, Ballantyne A, Berryman E, Fluet-Chouinard E, Jian J, Morris K A, Rey A and Vargas R 2024 Twenty years of progress, challenges, and opportunities in measuring and understanding soil respiration *J. Geophys. Res.* **129** e2023JG007637

Bradford M A, Davies C A, Frey S D, Maddox T R, Melillo J M, Mohan J E, Reynolds J F, Treseder K K and Wallenstein M D 2008 Thermal adaptation of soil microbial respiration to elevated temperature *Ecol. Lett.* **11** 1316–27

Brocca L, Melone F, Moramarco T and Morbidelli R 2010 Spatial-temporal variability of soil moisture and its estimation across scales *Water Resour. Res.* **46** W02516

Brown J H, Gillooly J F, Allen A P, Savage V M and West G B 2004 Toward a metabolic theory of ecology *Ecology* **85** 1771–89

Bruhn D *et al* 2022 Nocturnal plant respiration is under strong non-temperature control *Nat. Commun.* **13** 5650

Chen H Y, Xu X, Fang C M, Li B and Nie M 2021 Differences in the temperature dependence of wetland CO_2 and CH_4 emissions vary with water table depth *Nat. Clim. Change* **11** 766–71

Chen Y, Zhang Y, Zhang X, Stevens C, Fu S, Feng T, Li X, Chen Q, Liu S and Hu S 2024 Canopy and understory nitrogen additions differently affect soil microbial residual carbon in a temperate forest *Glob. Change Biol.* **30** e17427

Chu H *et al* 2023 AmeriFlux BASE data pipeline to support network growth and data sharing *Sci. Data* **10** 614

Davidson E A and Janssens I A 2006 Temperature sensitivity of soil carbon decomposition and feedbacks to climate change *Nature* **440** 165–73

Demyan M S *et al* 2016 Partitioning of ecosystem respiration in winter wheat and silage maize-modeling seasonal temperature effects *Agric. Ecosyst. Environ.* **224** 131–44

Dow C *et al* 2022 Warm springs alter timing but not total growth of temperate deciduous trees *Nature* **608** 552

Fouché J, Keller C, Allard M and Ambrosi J P 2014 Increased CO_2 fluxes under warming tests and soil solution chemistry in Histic and Turbic Cryosols, Salluit, Nunavik, Canada *Soil Biol. Biochem.* **68** 185–99

Grossiord C, Buckley T N, Cernusak L A, Novick K A, Poulter B, Siegwolf R T W, Sperry J S and McDowell N G 2020 Plant responses to rising vapor pressure deficit *New Phytol.* **226** 1550–66

IPCC 2022 *Global Warming of 1.5 °C: IPCC Special Report on Impacts of Global Warming of 1.5 °C above Pre-industrial Levels in Context of Strengthening Response to Climate Change, Sustainable Development, and Efforts to Eradicate Poverty* (Cambridge University Press) (https://doi.org/10.1017/9781009157940)

Jia X, Zha T S, Wu B, Zhang Y Q, Gong J N, Qin S G, Chen G P, Qian D, Kellomäki S and Peltola H 2014 Biophysical controls on net ecosystem CO_2 exchange over a semiarid shrubland in northwest China *Biogeosciences* **11** 4679–93

Johnston A S A *et al* 2021 Temperature thresholds of ecosystem respiration at a global scale *Nat. Ecol. Evol.* **5** 487–94

Li J Q, Pendall E, Dijkstra F A and Nie M 2020 Root effects on the temperature sensitivity of soil respiration depend on climatic condition and ecosystem type *Soil Tillage Res.* **199** 4

Li J, Pei J, Fang C, Li B and Nie M 2023 Opposing seasonal temperature dependencies of CO_2 and CH_4 emissions from wetlands *Glob. Change Biol.* **29** 1133–43

Liu X *et al* 2023 A new global C-band vegetation optical depth product from ASCAT: description, evaluation, and inter-comparison *Remote Sens. Environ.* **299** 113850

Liu Y L, Kumar M, Katul G G, Feng X and Konings A G 2020 Plant hydraulics accentuates the effect of atmospheric moisture stress on transpiration *Nat. Clim. Change* **10** 691

Liu Z H, Ballantyne A P, Poulter B, Anderegg W R L, Li W, Bastos A and Ciais P 2018 Precipitation thresholds regulate net carbon exchange at the continental scale *Nat. Commun.* **9** 10

Mahecha M D *et al* 2010 Global convergence in the temperature sensitivity of respiration at ecosystem level *Science* **329** 838–40

McDowell N G and Allen C D 2015 Darcy's law predicts widespread forest mortality under climate warming *Nat. Clim. Change* **5** 669–72

Moles A T *et al* 2014 Which is a better predictor of plant traits: temperature or precipitation? *J. Veg. Sci.* **25** 1167–80

Mu C C, Zhang T J, Zhao Q, Su H, Wang S F, Cao B, Peng X, Wu Q and Wu X 2017 Permafrost affects carbon exchange and its response to experimental warming on the northern Qinghai-Tibetan Plateau *Agric. For. Meteorol.* **247** 252–9

Niu B *et al* 2021 Warming homogenizes apparent temperature sensitivity of ecosystem respiration *Sci. Adv.* **7** 11

Niu S L *et al* 2012 Thermal optimality of net ecosystem exchange of carbon dioxide and underlying mechanisms *New Phytol.* **194** 775–83

Pastorello G *et al* 2020 The FLUXNET2015 dataset and the ONEFlux processing pipeline for eddy covariance data *Sci. Data* **7** 225

Pries C E H, van Logtestijn R S P, Schuur E A G, Natali S M, Cornelissen J H C, Aerts R and Dorrepaal E 2015 Decadal warming causes a consistent and persistent shift from heterotrophic to autotrophic respiration in contrasting permafrost ecosystems *Glob. Change Biol.* **21** 4508–19

Reichstein M *et al* 2005 On the separation of net ecosystem exchange into assimilation and ecosystem respiration: review and improved algorithm *Glob. Change Biol.* **11** 1424–39

Slot M and Kitajima K 2015 Whole-plant respiration and its temperature sensitivity during progressive carbon starvation *Funct. Plant Biol.* **42** 579–88

Sun W, Luo X Z, Fang Y Y, Shiga Y P, Zhang Y, Fisher J B, Keenan T F and Michalak A M 2023 Biome-scale temperature sensitivity of ecosystem respiration revealed by atmospheric CO_2 observations *Nat. Ecol. Evol.* **7** 1199

Tang R *et al* 2022 Increasing terrestrial ecosystem carbon release in response to autumn cooling and warming *Nat. Clim. Change* **12** 380–5

Tjoelker M G, Oleksyn J and Reich P B 2001 Modelling respiration of vegetation: evidence for a general temperature-dependent Q(10) *Glob. Change Biol.* **7** 223–30

Virtanen P *et al* 2020 SciPy 1.0: fundamental algorithms for scientific computing in Python *Nat. Methods* **17** 261–72

Yan Y, Piao S, Hammond W M, Chen A, Hong S, Xu H, Munson S M, Myneni R B and Allen C D 2024 Climate-induced tree-mortality pulses are obscured by broad-scale and long-term greening *Nat. Ecol. Evol.* **8** 912–23

Yang C J, Li G, Yan L J, Wu J Q, Li J, Liu S A and Lu Y H 2022 Effects of different vegetation types on ecosystem respiration in semiarid Loess Hilly Region, Central Gansu Province, China *Ecol. Indic.* **145** 11

Yu P, Zhou T, Luo H, Liu X, Shi P, Zhang Y, Zhang J, Zhou P and Xu Y 2022 Global pattern of ecosystem respiration tendencies and its implications on terrestrial carbon sink potential *Earth's Future* **10** e2022EF002703

Yuan W P *et al* 2019 Increased atmospheric vapor pressure deficit reduces global vegetation growth *Sci. Adv.* **5** eaax1396

Zhang T, Zhang Y J, Xu M J, Zhu J T, Chen N, Jiang Y B, Huang K, Zu J, Liu Y and Yu G 2018 Water availability is more important than temperature in driving the carbon fluxes of an alpine meadow on the Tibetan Plateau *Agric. For. Meteorol.* **256** 22–31

Zhang Y *et al* 2024 Exploring the ecological meanings of temperature sensitivity of ecosystem respiration from different methods *Sci. Total Environ.* **923** 171403

Zhang Z Y *et al* 2023 Large diurnal compensatory effects mitigate the response of Amazonian forests to atmospheric warming and drying *Sci. Adv.* **9** 15